

In Vivo Structural Changes after CXL

International CXL Experts' Meeting

Hotel Mövenpick Airport
Zurich - December 2-3,
2016

Cosimo Mazzotta MD, PhD

Assistant Professor Post-Graduate Ophthalmology School
Department of Medicine, Surgery and Neurosciences, Ophthalmology Unit
University of Siena, Italy

Director Siena International Crosslinking Center®

cgmazzotta@libero.it

www.mazzottacosimo.com

Author declare no financial interest

In Vivo Confocal Microscopy after Corneal Collagen Crosslinking

COSIMO MAZZOTTA, MD, PhD,¹ FARHAD HAFEZI, MD, PhD,² GEORGE KYMIONIS, MD, PhD,³
STEFANO CARAGIULI, MD,¹ SOOSAN JACOB, MD, PhD,⁴ CLAUDIO TRAVERSI, MD,¹
STEFANO BARABINO, MD,⁵ AND J. BRADLEY RANDLEMAN, MD⁶

Review

THE OCULAR SURFACE / OCTOBER 2015, VOL. 13 NO. 4 / www.theocularsurface.com

Table 3. Summary of in vivo confocal microscopy findings after conventional CXL

Author	Country	Treatment	Design	N. of eyes	Follow-up (months)	Epithelial healing (days)	Nerves regeneration (months)	Keratocytes repopulation (months)	Endothelium
Mazzotta et al. 2006	Italy	CXL	qualitative	10	6	5	6	n.a.	Unaltered
Mazzotta et al. 2007	Italy	CXL	qualitative	10	6	4	6	6	Unaltered
Mazzotta et al. 2008	Italy	CXL	qualitative	44	36	4	12	6	Unaltered
Kymionis et al. 2009	Greece	CXL	qualitative	10	6	4	6	6	Unaltered
Croxatto et al. 2010	Argentina	CXL	qualitative	18	36	4	6	6	Unaltered
Knappe et al. 2011	Germany	CXL	qualitative	8	12	14	12	6	Unaltered
Caporossi et al. 2012	Italy	TE-CXL	qualitative	10	6	4	no nerve loss	unchanged	Unaltered
Toboul et al. 2012	France	TE-CXL	qualitative	8	6	3	no nerve loss	unchanged	Unaltered
Jordan et al. 2014	N. Zealand	CXL	quantitative	38	12	n.a.	12 (to baseline values)	12 (to baseline values)	Unaltered
Sharma et al. 2015	India	CXL	qualitative	23	6	7	6	6	Unaltered

n. a., not available; CXL, conventional epithelium-off CXL; TE-CXL, transepithelial CXL.

Epithelium

CXL
LIMBUS

EPI-OFF
CXL 3 mW
ACXL 9-30 mW

EPI-ON
CXL 3-10 mW
ACXL 45 mW

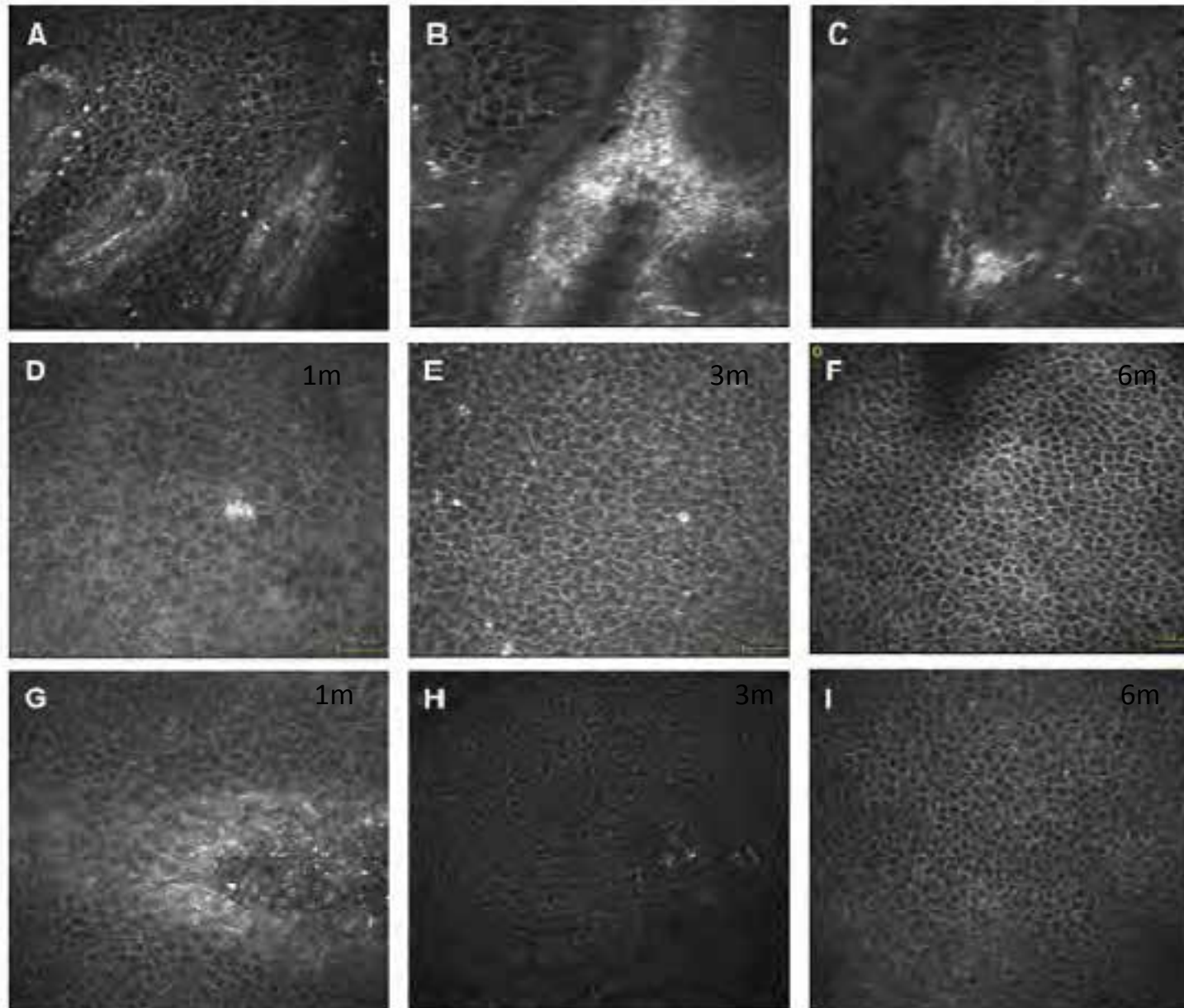


Figure 8. ICM analysis of limbal structures (Vogt's palisades) of the cornea after conventional CXL did not show pathological micromorphological changes in limbal stem cells line. Basal limbal epithelial cells (bright particles spreading from coronal germinal epithelium of limbal Vogt palisades) divide and migrate (A-C) toward the center in a centripetal migration pattern and later to the surface. ICM of epithelium after conventional CXL at first postoperative month (D) showed irregular cell borders with hyper-reflective spots. Postoperative stratification of basal epithelium improving corneal optical properties at 3rd postoperative month (E) and optimized mosaic quality at 6th postoperative month (F). ICM after TE-CXL showed immediate diffuse necrotic areas devoid of epithelial cells and hyper-reflecting spots (apoptotic bodies; image G). Three months after treatment, mosaic pattern and cell borders are visible (H). Between the 3rd and 6th months, the epithelium resembled preoperative conditions (I).

Epithelium regenerates
Into 72 hours

Stratification and thickness
Requires 1-3 months

Epi-on damage epithelium
Chemical and radiative

Sometimes chronic postoperative
epitheliopathy

Nerves

EPI-OFF

EPI-ON
ACXL
45mW

EPI-ON
CXL
3mW
10 mW

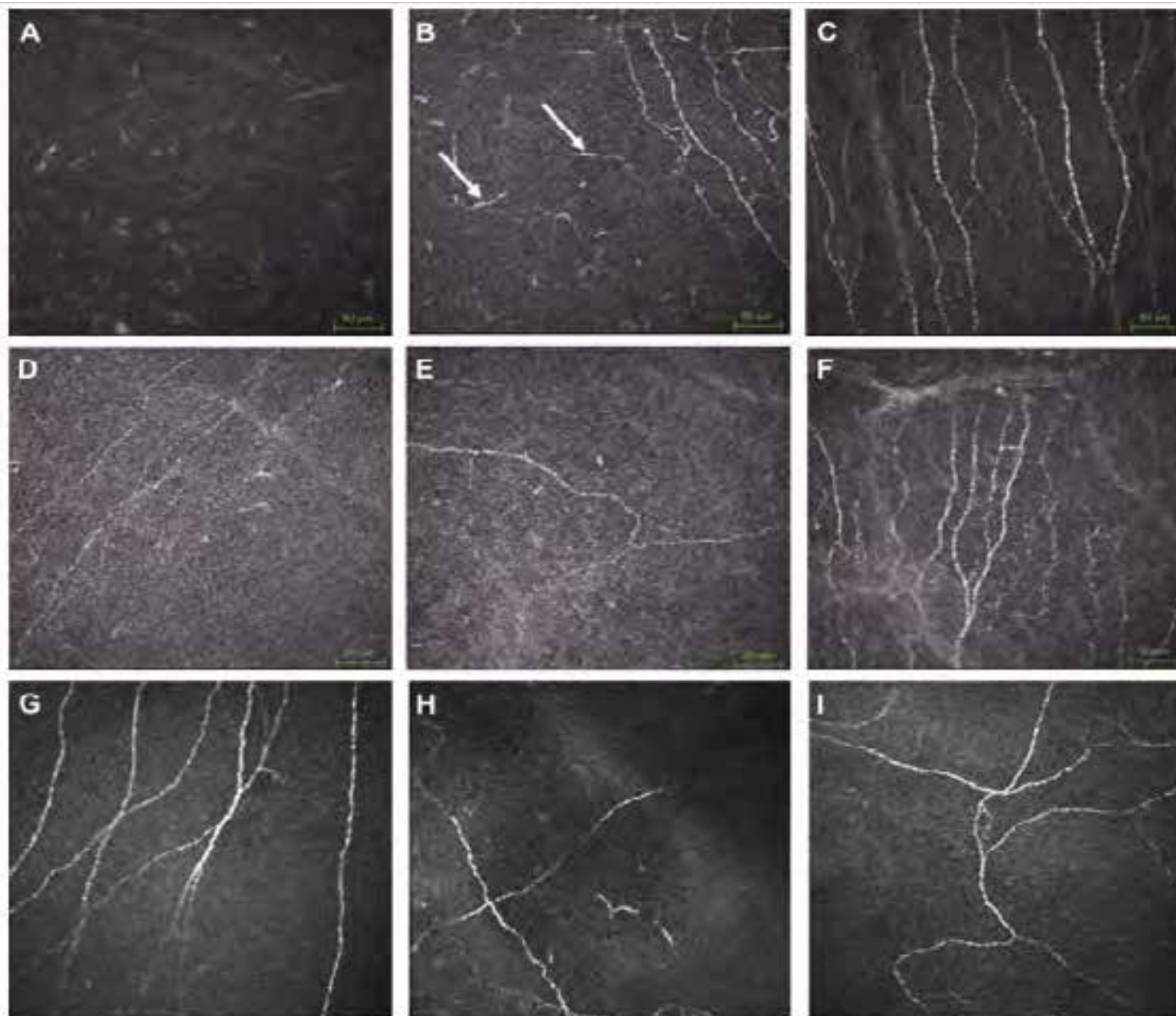


Figure 9. IVCM after conventional CXL and ACXL showed identical features with immediate disappearance of subepithelial plexus (SEP) nerve fibers (A). Regeneration started rapidly and subepithelial nerve flocculation simulated the presence of dendritic cells: "pseudo-dendritic nerves regeneration" (B, white arrows). Regeneration of nerve fibers was almost complete 6 months after the operation, with fully restored corneal sensitivity (C). IVCM after TE-ACXL with high intensity UV-A power (45 mW/cm²) determined a nerve loss similar to that with conventional CXL (D) followed by gradual nerve regeneration of disconnected fibers (E) followed by interconnected fibers after the 6th month (F). IVCM after TE-CXL showed that SEP nerves did not disappear (G). Similarly, SEP nerves were present in subsequent follow-up scans (H and I).

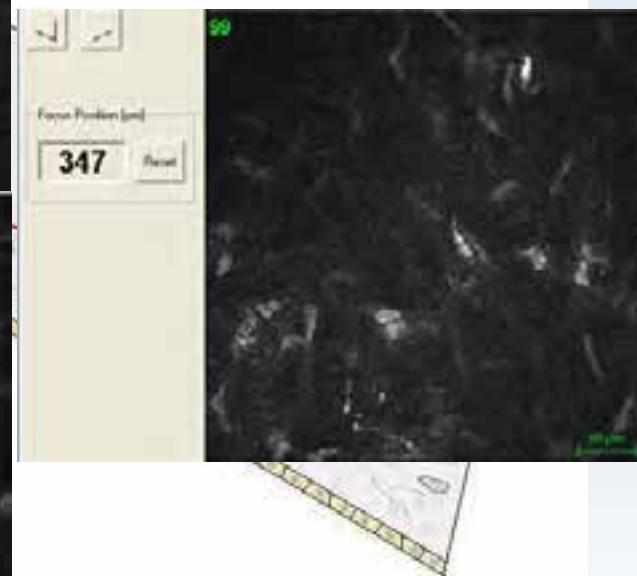
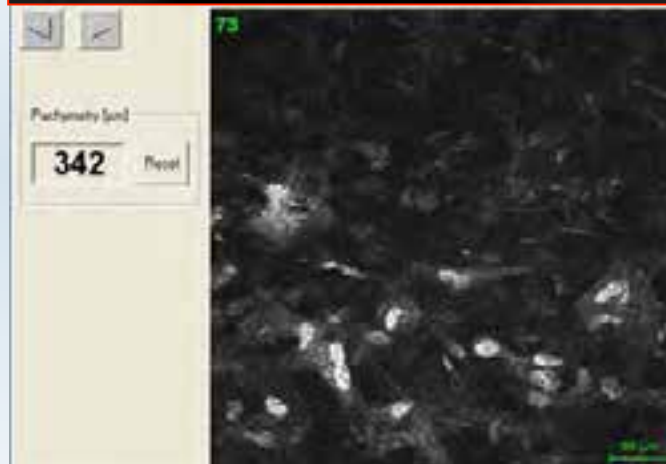
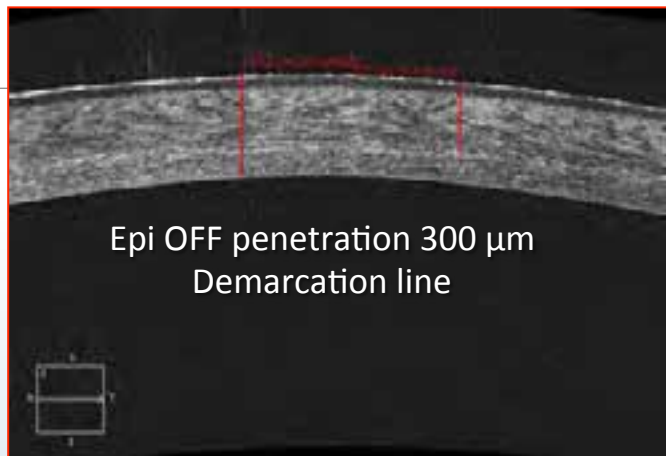
Immediate Nerve loss
Regeneration by sprouting
Nerve fibers at 1 month
Completing between
6 and 12 months
Regular corneal sensitivity

SEP nerves damage observed
after very high irradiation
Epi on 45 mW despite
Epithelium on

Undamaged SEP nerves
After conventional and
High irradiance epi-
CXL (TE and I-CXL)

Keratoconus and Keratocytes

Epi-Off CXL



Treatment of Progressive Keratoconus by Riboflavin-UVA-Induced Cross-Linking of Corneal Collagen

*Ultrastructural Analysis by Heidelberg Retinal Tomograph
In Vivo Confocal Microscopy in Humans*

Cosimo Mazzotta, PhD, Angelo Balestrazzi, PhD,* Claudio Traversi, MD,* Stefano Baiocchi, MD,* Tomaso Caporossi, MD,† Cristina Tommasi, MD,* and Aldo Caporossi, MD**

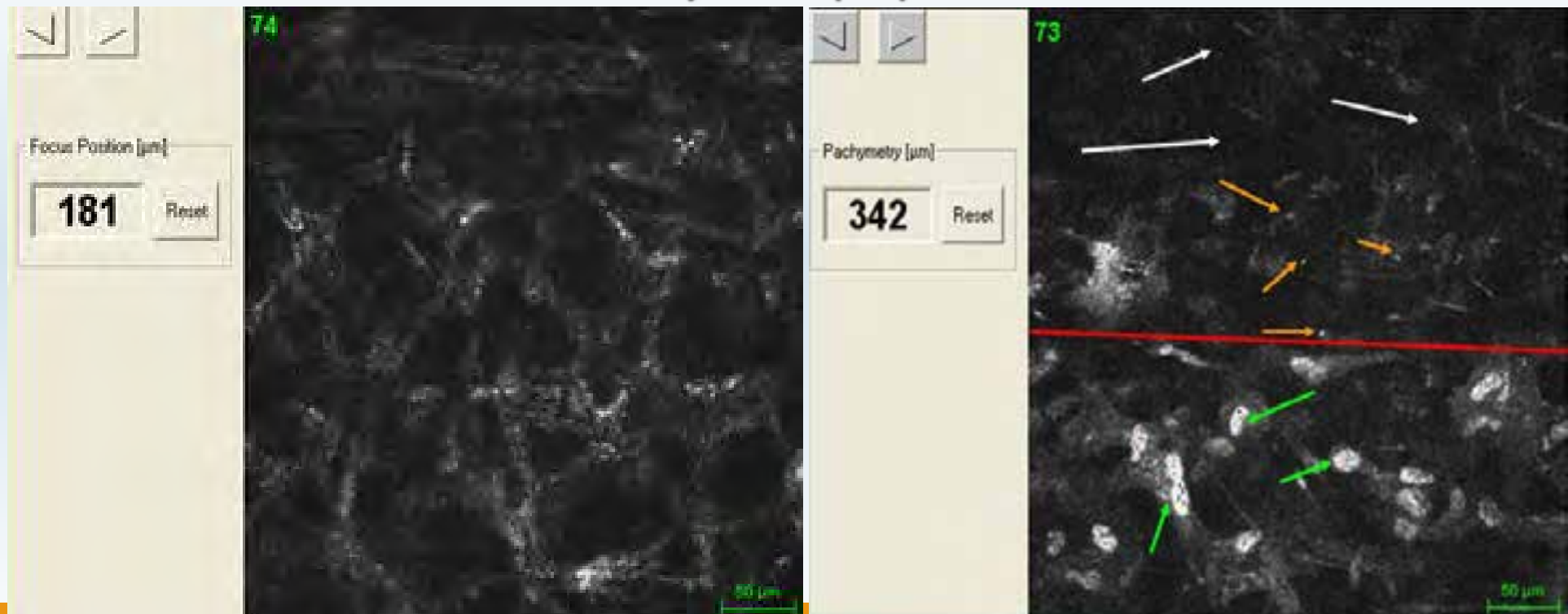
Corneal Healing After Riboflavin Ultraviolet-A Collagen Cross-Linking Determined by Confocal Laser Scanning Microscopy In Vivo: Early and Late Modifications

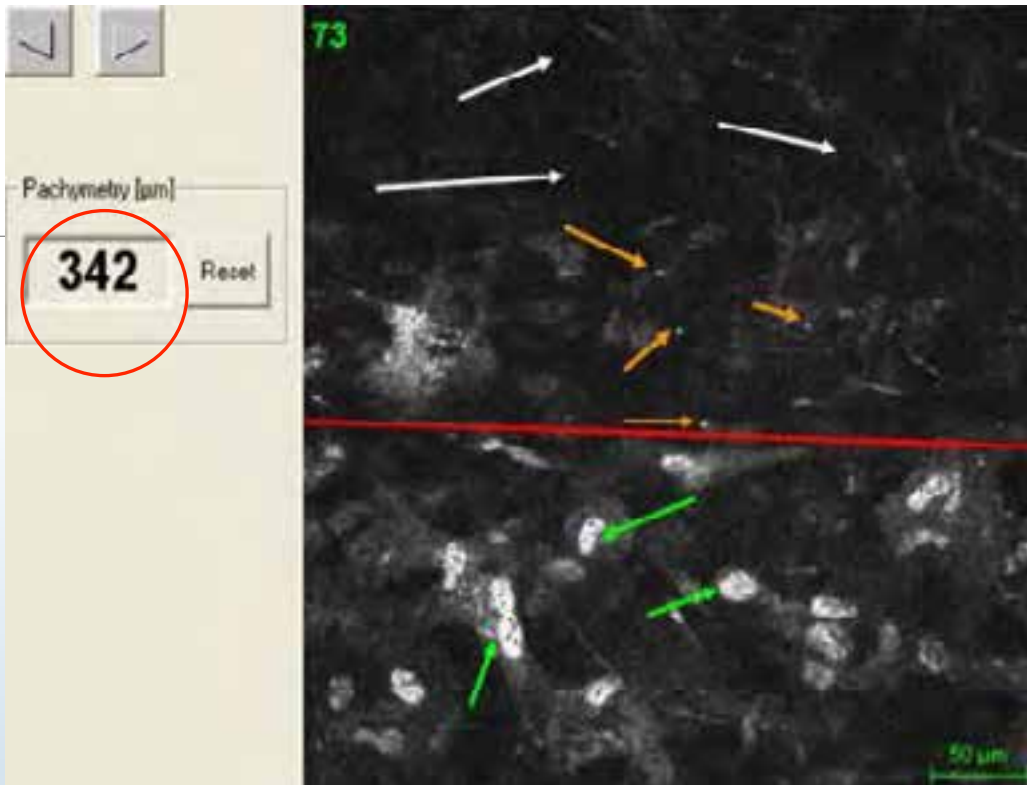
AMERICAN JOURNAL OF OPHTHALMOLOGY

APRIL 2010

COSIMO MAZZOTTA, CLAUDIO TRAVERSI, STEFANO BAIOCCHI, ORSOLA CAPOROSSI, CRISTINA BOVONE, MARIA CATERINA SPARANO, ANGELO BALESTRAZZI, AND ALDO CAPOROSSI

Keratocytes Apoptosis





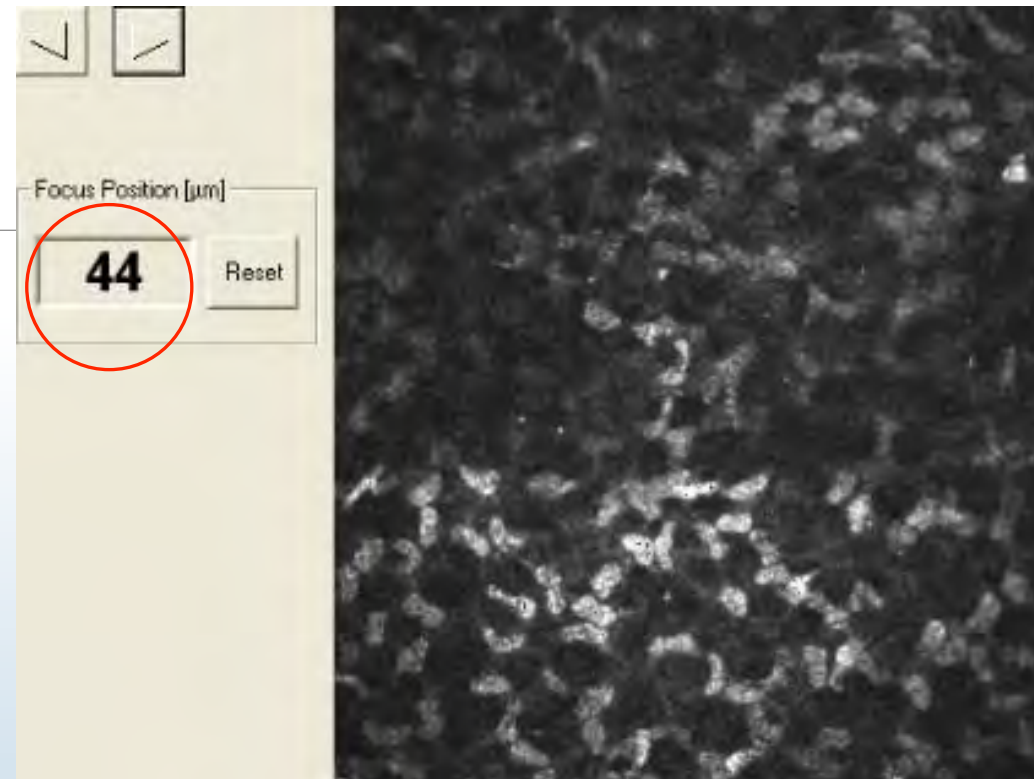
CLINICAL SCIENCE

Cornea. 2007 May;26(4):390-7

Treatment of Progressive Keratoconus by Riboflavin-UVA-Induced Cross-Linking of Corneal Collagen

Ultrastructural Analysis by Heidelberg Retinal Tomograph II In Vivo Confocal Microscopy in Humans

Cosimo Mazzotta, PhD,* Angelo Balestrazzi, PhD,* Claudio Traversi, MD,* Stefano Baiocchi, PhD,* Tomaso Caporossi, MD,† Cristina Tommasi, MD,* and Aldo Caporossi, MD*



ORIGINAL ARTICLE

Eur J Ophthalmol. 2012 Jul;22 Suppl 7:81-8.

Transepithelial corneal collagen crosslinking for keratoconus: qualitative investigation by in vivo HRT II confocal analysis

Aldo Caporossi[†], Cosimo Mazzotta[†], Stefano Baiocchi[†], Tomaso Caporossi[†], Anna Lucia Paradiso[†]

[†]Department of Ophthalmology, Siena University, Siena - Italy

[†]Department of Ophthalmology, Roma Catholic University, Rome - Italy

IVCM AFTER CORNEAL COLLAGEN CROSSLINKING / Mazzotta, et al

Table 2. Demarcation line depth

CXL Treatments 84 eyes	Conventional CXL 44 eyes 3 mW	C-light ACXL 10 eyes 30 mW	P-light ACXL 10 eyes 30 mW	TE CXL 10 eyes 3 mW	TE ACXL 10 eyes 45 mW
Average demarcation line depth (measured from epithelial surface)	350 ± 20 μm	200 ± 20 μm	250 ± 20 μm	100 ± 20 μm	100 ± 20 μm

*Average epithelial thickness: 50 ± 10 μm.

CXL, conventional crosslinking; C-light ACXL, continuous light accelerated crosslinking; P-light ACXL, pulsed light accelerated crosslinking;

TE CXL, transepithelial crosslinking; TE ACXL, transepithelial accelerated crosslinking.

THE OCULAR SURFACE / OCTOBER 2015, VOL. 13 NO. 4 / www.theocularsurface.com

IVCM AFTER CORNEAL COLLAGEN CROSSLINKING / Mazzotta, et al

CXL 3 mW
Epi-Off

CXL 30 mW
Epi-Off

CXL 3mW
Epi-On

ACXL 30 mW
Pulsed Epi-Off

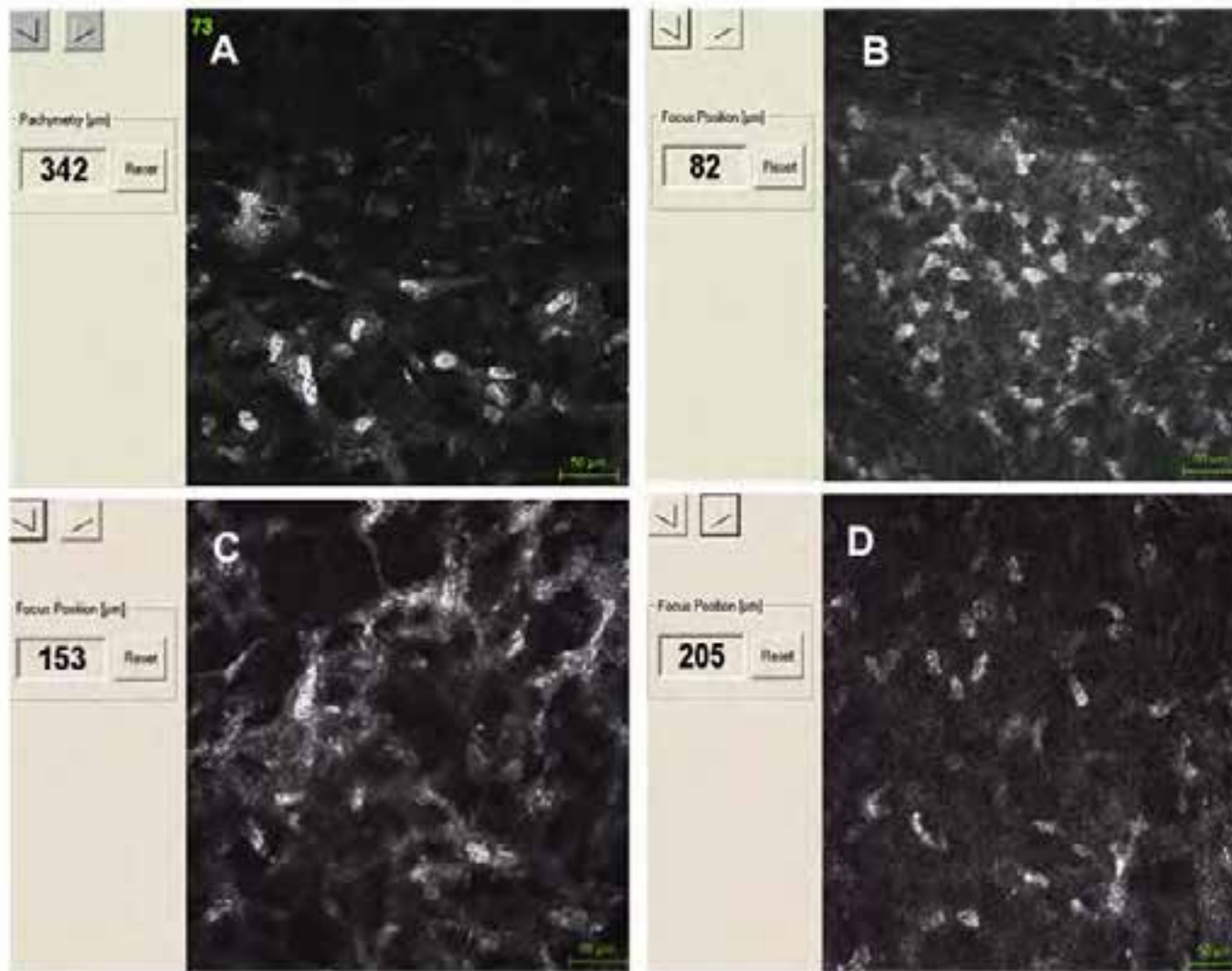
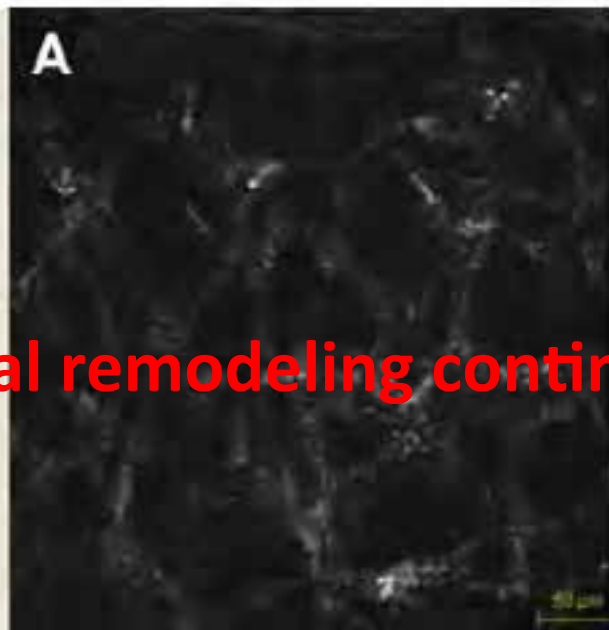


Figure 1. Demarcation lines occurring with various techniques. A: Conventional CXL shows a penetration of keratocyte apoptosis at 350 μm measured from epithelial surface. B: TE-CXL shows a limited apoptosis under 100 μm. ACXL with continuous light shows keratocyte apoptosis at 150 μm (C) and ACXL with pulsed light at 200 μm (D).

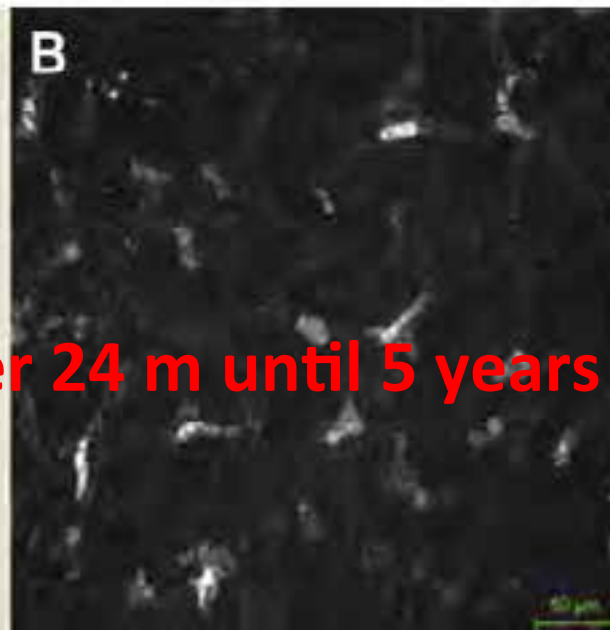
Normal remodeling continues over 24 m until 5 years

ost

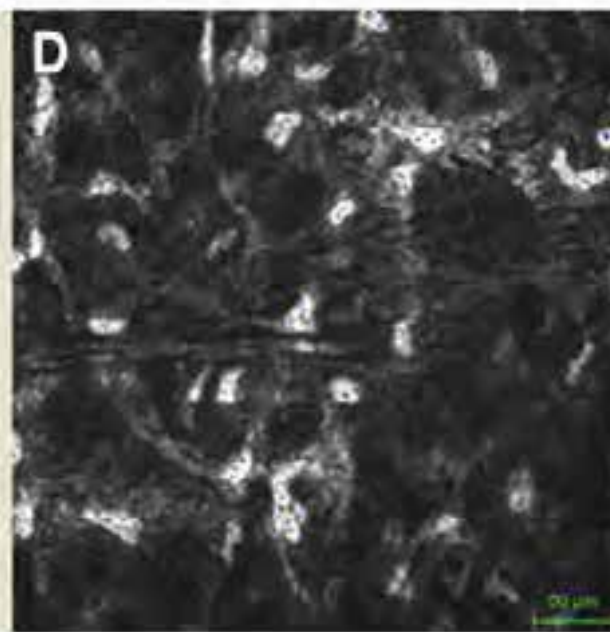
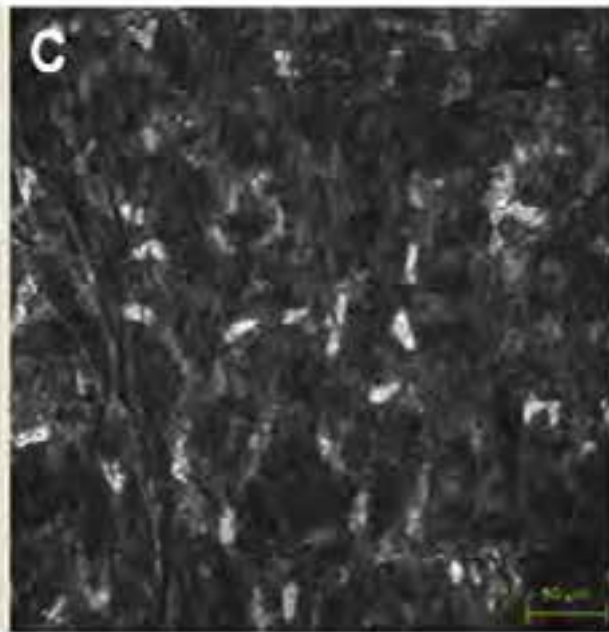
ost



3m post



12m post



Conventional CXL

Figure 3. IVCM after conventional CXL demonstrated in vivo in humans keratocyte apoptosis followed by progressive repopulation of the anterior-mid stroma. Lacunar edema is visible in the first postoperative month with trabecular patterned hyperdense tissue surrounding edematous areas, entrapping apoptotic keratocyte bodies (A). At the 3rd postoperative stromal edema was reduced and keratocyte repopulation began, confirmed by the presence of keratocyte-activated nuclei (B). Six months after treatment, edema disappeared, followed by hyper-reflective extracellular matrix and cell repopulation (C). One year after treatment, anterior-mid stroma was repopulated by keratocytes and surrounded by dense extracellular collagen tissue (D).

IVCM AFTER CORNEAL COLLAGEN CROSSLINKING / Mazzotta, et al

THE OCULAR SURFACE / OCTOBER 2015, VOL. 13 NO. 4 / www.theocularsurface.com

Table 1. Quantitative analysis of keratocyte density after CXL, ACXL, TE CXL and TE ACXL

Keratocyte/mm ² 100 μm depth	Pre op	1 m	6 m	12 m	24 m
CXL 24 eyes	588 ± 39	no	444 ± 38	589 ± 34	622 ± 44
ACXL 20 eyes	464 ± 72	no	359 ± 34	450 ± 40	446 ± 39
TE CXL 10 eyes	502 ± 42	489 ± 30	511 ± 42	601 ± 35	599 ± 41
TE ACXL 10 eyes	699 ± 35	594 ± 32	690 ± 65	804 ± 69	769 ± 52

CXL, conventional CXL 3mW/cm²; ACXL, accelerated crosslinking 30 mW/cm²; TE CXL, transepithelial crosslinking 3 mW/cm²; TE ACXL, transepithelial accelerated crosslinking 45 mW/cm².

Pulsed vs continuous light accelerated corneal collagen crosslinking: *in vivo* qualitative investigation by confocal microscopy and corneal OCT

Pulsed light increase apoptosis penetration 50 +/- 20 micra

C Mazzotta¹, C Traversi¹, S Caragiuli¹ and M Rechichi²

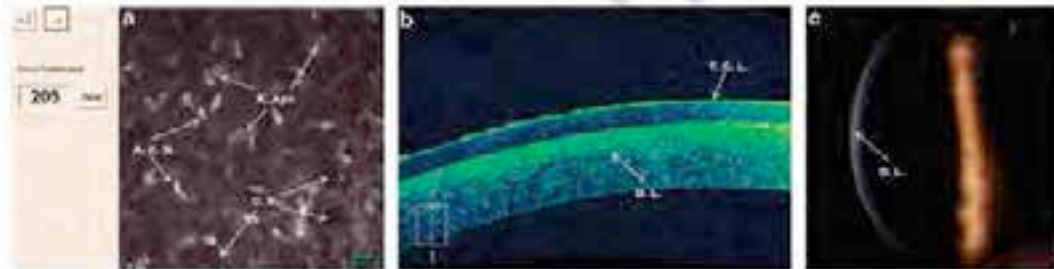


Figure 1 Pulsed light accelerated crosslinking (PL-ACXL) confocal scan reveals keratocytes apoptosis (K. Apo), lacunar corneal edema (C.E.), and activated keratocytes nuclei (A.K.N.) with a mean penetration of 200 μm (a); spectral domain corneal OCT performed before removing therapeutic contact lens after treatment (T.C.L.) reveals an increased reflectivity of the anterior mid-stroma after treatment with an inhomogeneous demarcation line (D.L.) at 180 μm of depth (b); slit lamp examination at first postoperative month reveals a visible demarcation line (D.L.) (c).

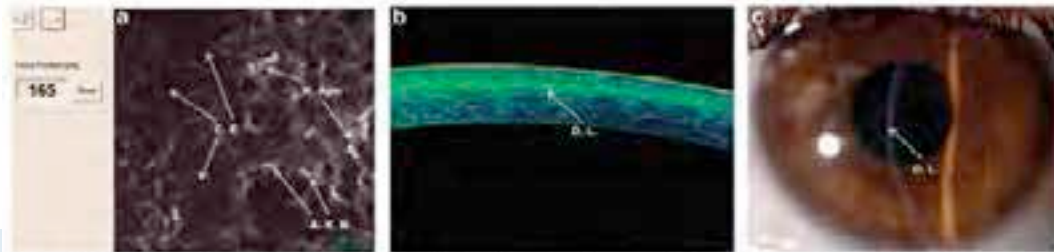


Figure 2 Continuous light accelerated crosslinking (CL-ACXL) confocal scan reveals keratocytes apoptosis (K. Apo), lacunar corneal edema (C.E.), and activated keratocytes nuclei (A.K.N.) with a mean penetration of 160 μm (a); spectral domain corneal OCT performed after therapeutic contact lens removal reveals an increased reflectivity of the anterior mid-stroma after treatment with an inhomogeneous demarcation line (D.L.) at 160 μm of depth (b); slit lamp examination at first postoperative month reveals a visible demarcation line (D.L.) (c).

CLINICAL STUDY

[Pulsed vs continuous light accelerated corneal collagen crosslinking: *in vivo* qualitative investigation by confocal microscopy and corneal OCT.](#)

Mazzotta C, Traversi C, Caragiuli S, Rechichi M.

Eye (Lond). 2014 Jul 25. doi: 10.1038/eye.2014.163.

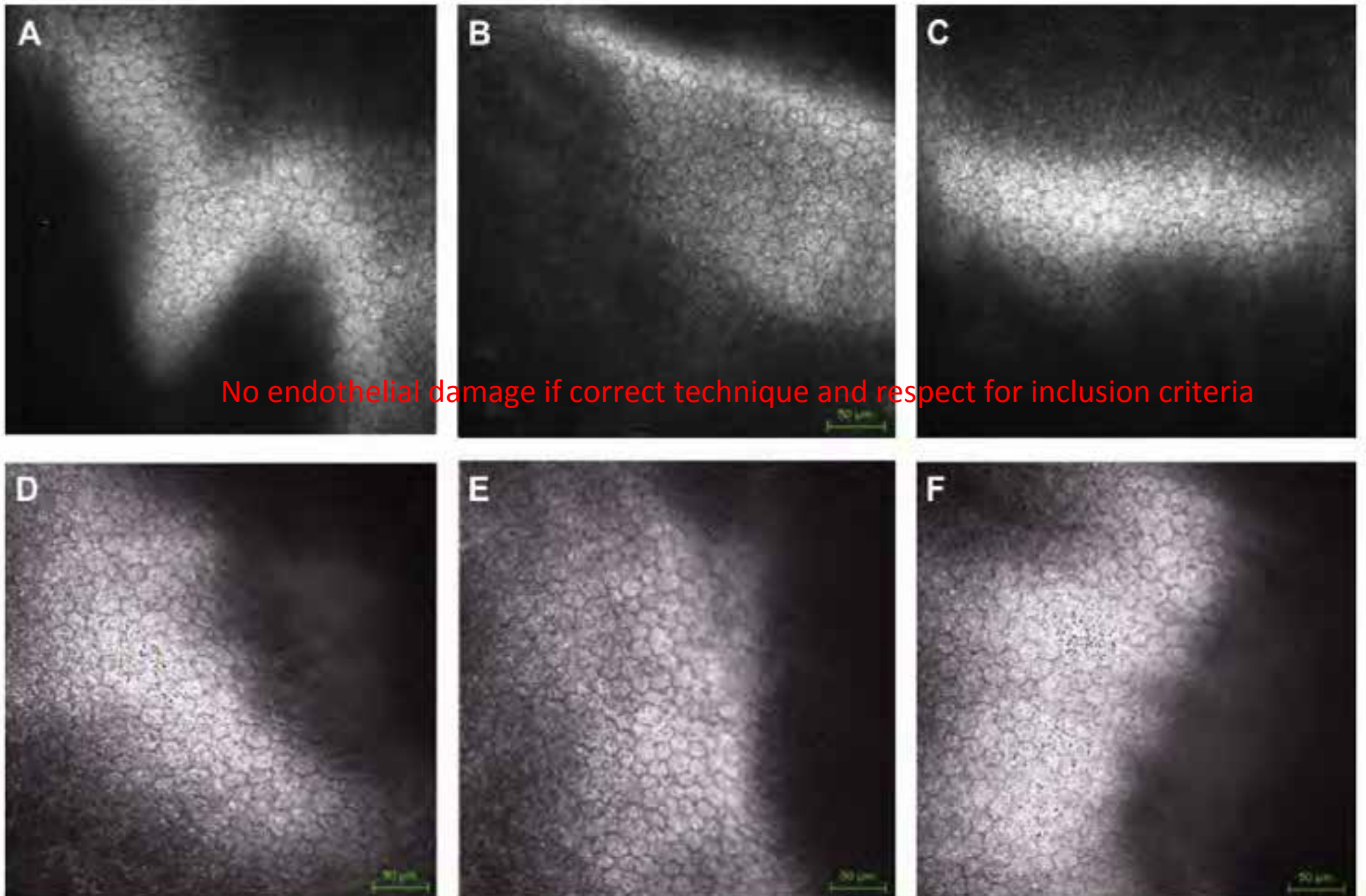


Figure 10. ICM analysis at current state-of-the-art conventional CXL at 1-year (A), 3-year (B) and 5-year (C) follow-up and ACXL after 6-month (D), 1-year (E), and 18-month (F) follow-up confirmed the safety of the treatments, without morphological or functional alterations of the corneal endothelium. The endothelial cell reduction observed after treatment was 2% per year on average.

Clinical Study

Accelerated Corneal Collagen Cross-Linking Using Topography-Guided UV-A Energy Emission: Preliminary Clinical and Morphological Outcomes

Cosimo Mazzotta,^{1,2} Antonio Moramarco,³ Claudio Traversi,² Stefano Baiocchi,² Alfonso Iovieno,³ and Luigi Fontana³

¹*Siena Int. Cross-Linking Center, Siena, Italy*

²*Department of Medical, Surgical and Neurosciences, Ophthalmology Unit, Siena University, Siena, Italy*

³*Ophthalmology Unit, Arcispedale Santa Maria Nuova Hospital-IRCCS, Reggio Emilia, Italy*

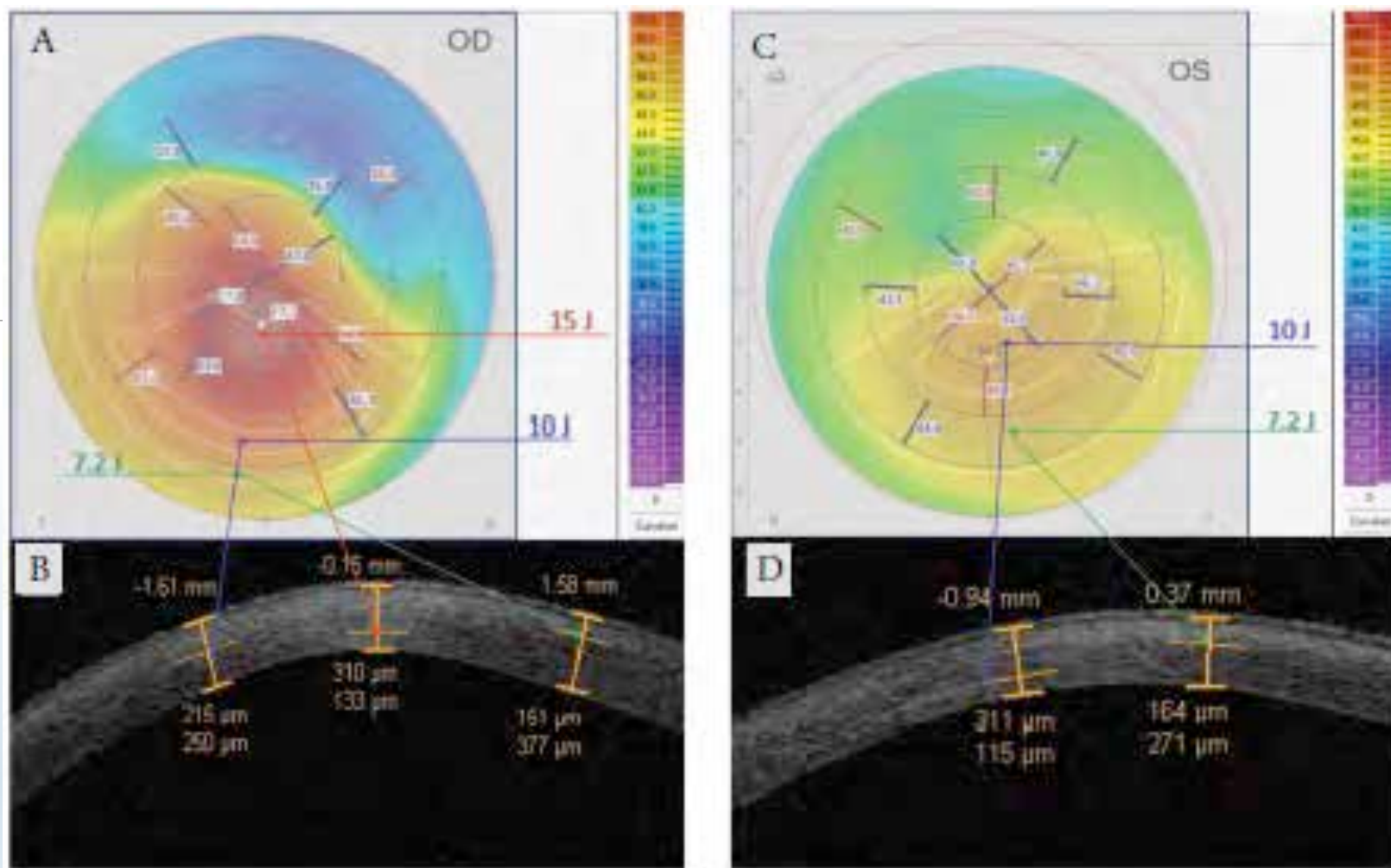
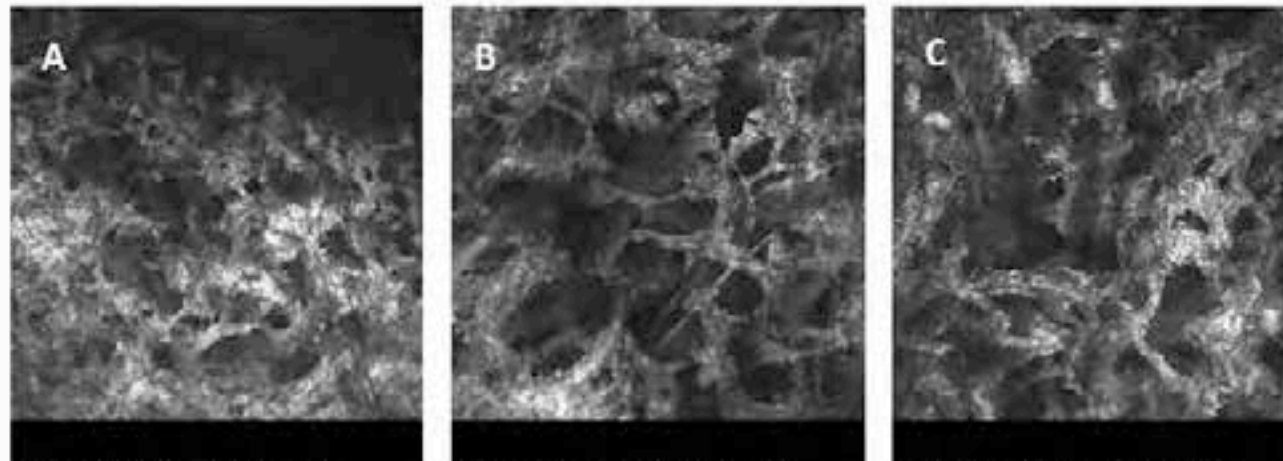
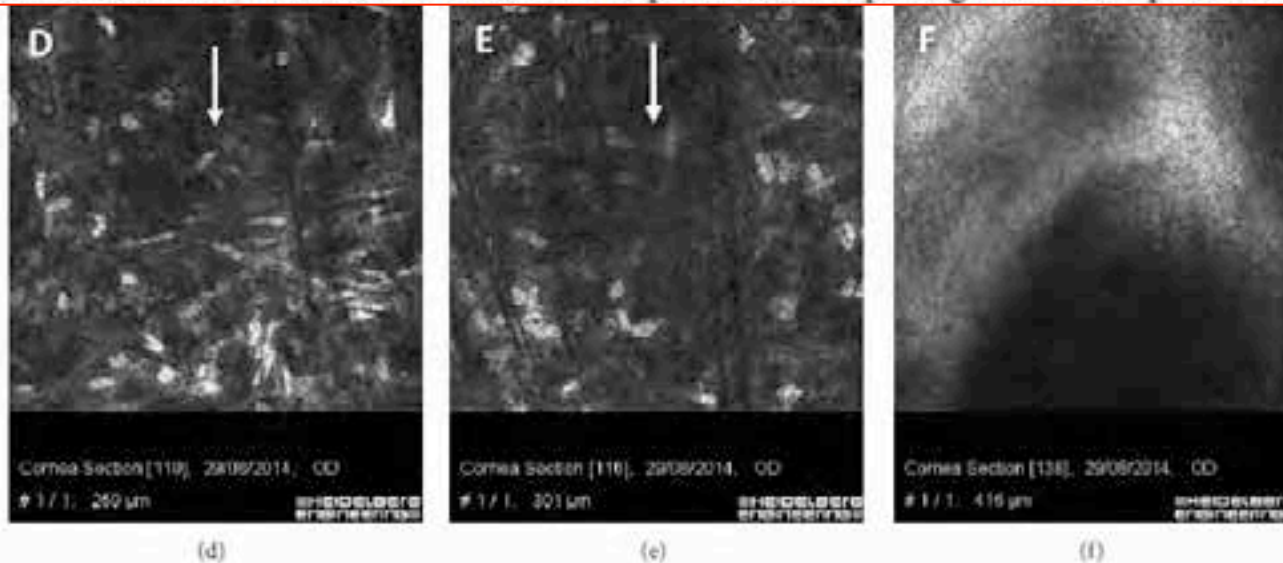


FIGURE 5: Topography-guided ACXL treatment programs according to different KC severity. (a) shows a 3-Zone topography-guided ACXL treatment planning according to corneal curvatures. Postoperative OCT scans one month after treatment (b) revealed a triple demarcation line according to the three different exposure times and energy doses: $7.2 \text{ J}/\text{cm}^2$ in the peripheral KC flattest area 48 D and under (depth $151 \mu\text{m}$), green arrows (8 min UV-A exposure); $10 \text{ J}/\text{cm}^2$ in the intermediate area between 48 and 52 D (depth $215 \mu\text{m}$), blue arrows (11 min UV-A exposure); $15 \text{ J}/\text{cm}^2$ in the steepest area (depth $310 \mu\text{m}$), red arrows (16 min UV-A exposure). (c) shows a 2-Zone topography-guided ACXL treatment with $7.2 \text{ J}/\text{cm}^2$ (green arrows) and $10 \text{ J}/\text{cm}^2$ (blue arrows) E doses treatment planning. OCT scan performed one month after treatment (d) revealed a double demarcation line according to the different exposure times and doses delivered according to corneal curvatures, reaching a demarcation line depth of $164 \mu\text{m}$ in the peripheral area treated with $7.2 \text{ J}/\text{cm}^2$ for 8 min of UVA exposure (green arrow) and $311 \mu\text{m}$ in the steeper paracentral area treated with $10 \text{ J}/\text{cm}^2$ for 11 min of UV-A exposure (blue arrow).



ECM Reflectivity
Changes
Linearly with the
Dose

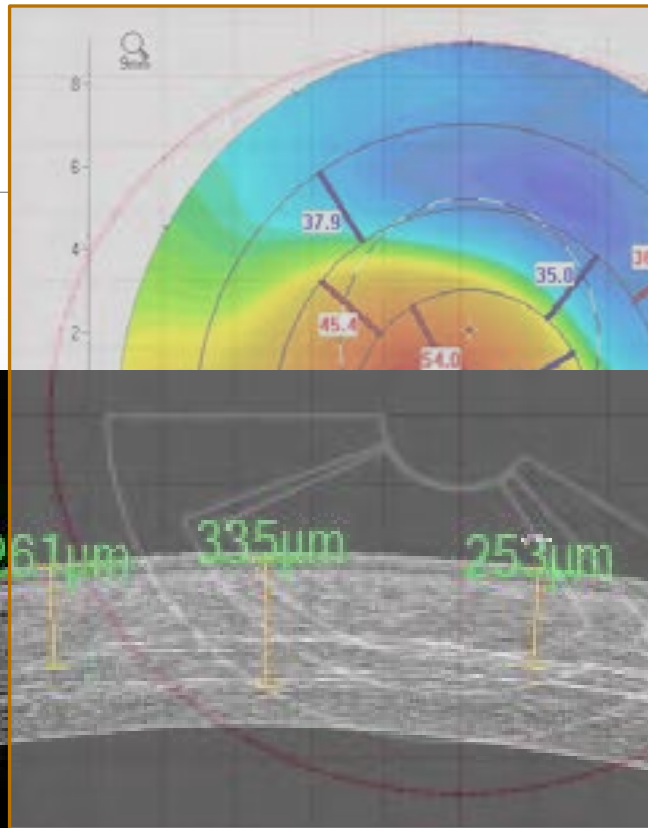
Preliminary results show correspondence between the energy dose applied and the microstructural stromal changes induced by the cross-linking at various depths in different areas of treated cornea. One year after surgery a significant reduction in the topographic astigmatism and comatic aberration was detected. None of the patients developed significant complications.



Apoptosis increases
Rising the E dose
Over 7.2 J

FIGURE 6: IVCM scans in the first month after high-irradiance topography-guided CXL. Different demarcation lines were documented at 150 µm depth in the flattest areas (48 D and under) irradiated at 7.2 J/cm² ((a), (b), and (c)); at 250 µm depth in the area (>48 D and <52 D) irradiated at 10 J/cm² E dose (d); at 300 µm depth in the steepest cone area (>52 D) irradiated at 15 J/cm² E dose (e). IVCM also showed hyperreflectivity of corneal tissue and keratocytes apoptosis associated with dense trabecular patterned lacunar edema and nerve disappearance ((a), (b), and (c)). No endothelial damage was documented (f).

CXL MULTIPLE DEMARCATION LINES



3-Zone topography-guided ACXL



deeper demarcation line in the “high energy” zone. The observed reduction of astigmatism may result from the shorter irradiation time. However, considering that the depth of the conventional CXL (C-CXL) with 5.4 J/cm^2 dose and 30 minutes of total UV-A exposure time reached $300 \mu\text{m}$ of demarcation on average [19], the topography-guided accelerated CXL achieved a comparable treatment penetration in 18 minutes instead of 30 minutes and in this contest the higher dose may be a possible explanation of the increased treatment penetration beyond the exposure time.

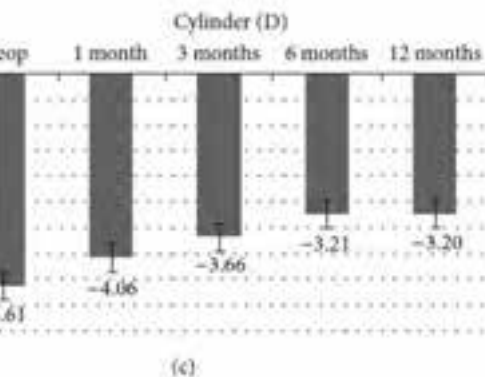
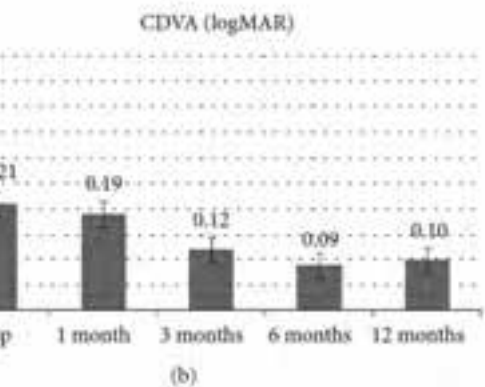
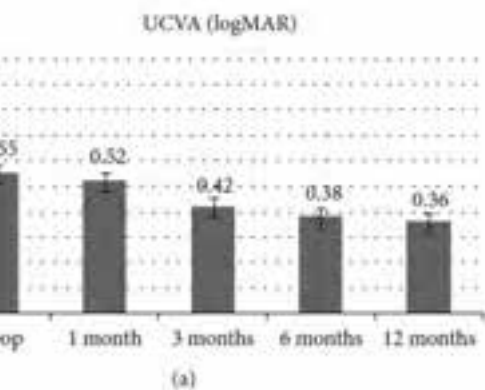


Figure 4: Corneal OCT following high-irradiance topography-guided CXL. At 3rd postoperative month (a), multiple demarcation lines due to the different energy doses delivered according to the topography-guided CXL protocol were evident. (b) illustrates the topography-guided treatment in progress. (c) shows the topo-guided treatment planning with programmed double energy dose: 7.2 J/cm² in the flattest area under 48 D (yellow arrow) with arc-step pattern, and 10 J/cm² in the steepest central area over 48 D (red arrow) with circular pattern. (d) shows the 12th month postoperative flattening compared with preoperative tomography (e), followed by compensatory steepening of the flattest superior cornea documented in differential corneal tomography (f).

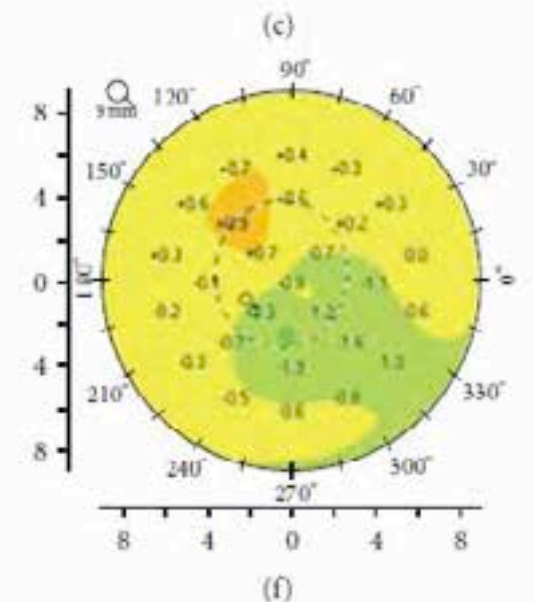
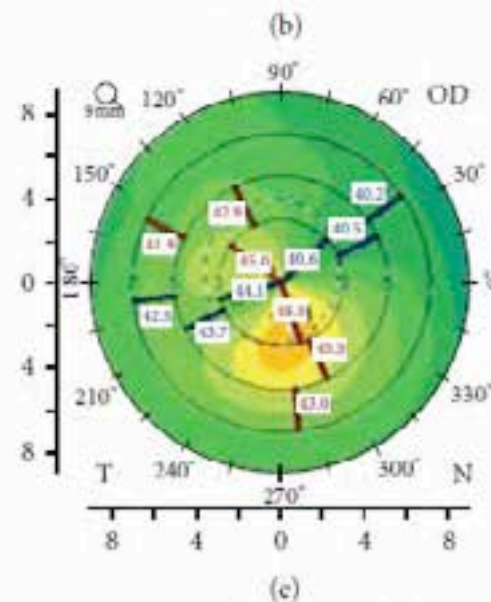
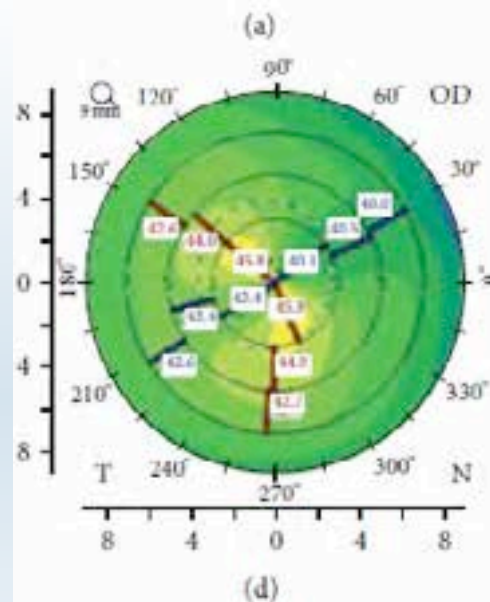
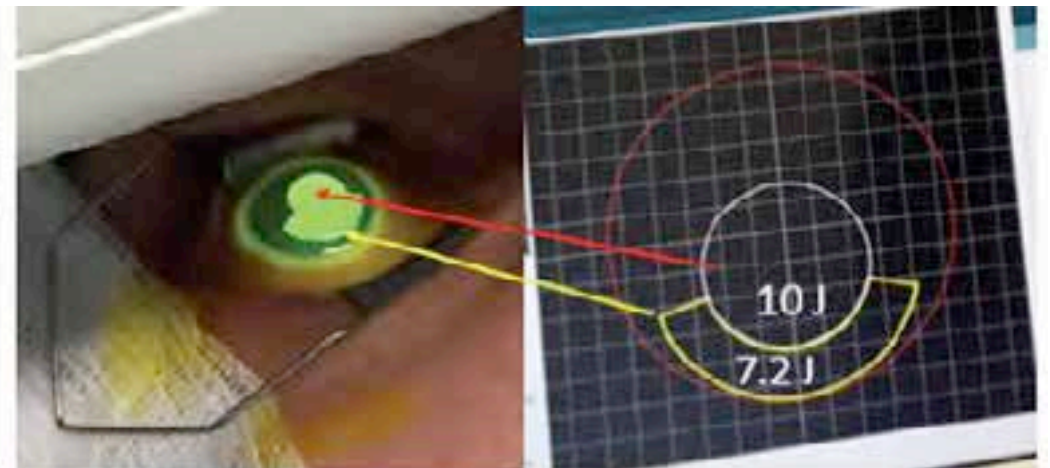
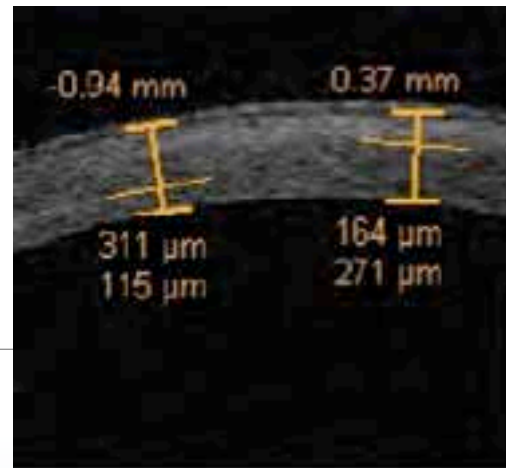


Figure 4: Corneal OCT following high-irradiance topography-guided CXL. At 3rd postoperative month (a), multiple demarcation lines due to the different energy doses delivered according to the topography-guided CXL protocol were evident. (b) illustrates the topography-guided treatment in progress. (c) shows the topo-guided treatment planning with programmed double energy dose: 7.2 J/cm² in the flattest area under 48 D (yellow arrow) with arc-step pattern, and 10 J/cm² in the steepest central area over 48 D (red arrow) with circular pattern. (d) shows the 12th month postoperative flattening compared with preoperative tomography (e), followed by compensatory steepening of the flattest superior cornea documented in differential corneal tomography (f).

Proposed Efficacy Study of High Versus Standard Irradiance of Fractionated Riboflavin/Ultraviolet A Cross-Linking With Equivalent Energy Exposure

Ronald R. Krueger, M.D., Satish Herekar, M.S., and Eberhard Spoerl, Ph.D.

Stress at the other equidose irradiances of 2, 9, 15 continuously, and 15 W/cm² fractionated were 140±21.9, 162.8±70, 154.1±70, and 164.1±64×10³ N/m², respectively. When comparing the irradiances of 15 W/cm² continuously and fractionated to the standard irradiation, the difference was not statistically different (*P*=0.799 and 0.643), respectively.

Conclusion: High irradiance riboflavin/UVA cross-linking with equivalent energy exposure demonstrates comparable efficacy in stiffening corneal collagen when with standard irradiance, but with considerably less exposure time.

Accelerated Crosslinking Photo-chemical Basis The Bunsen-Roscoe Law of Reciprocity

J. Physiol. (1904) 218, 137-140

THE BUNSEN-ROSCOE LAW FOR THE HUMAN EYE
AT VERY SHORT DURATIONS

By G. S. BRINDLEY

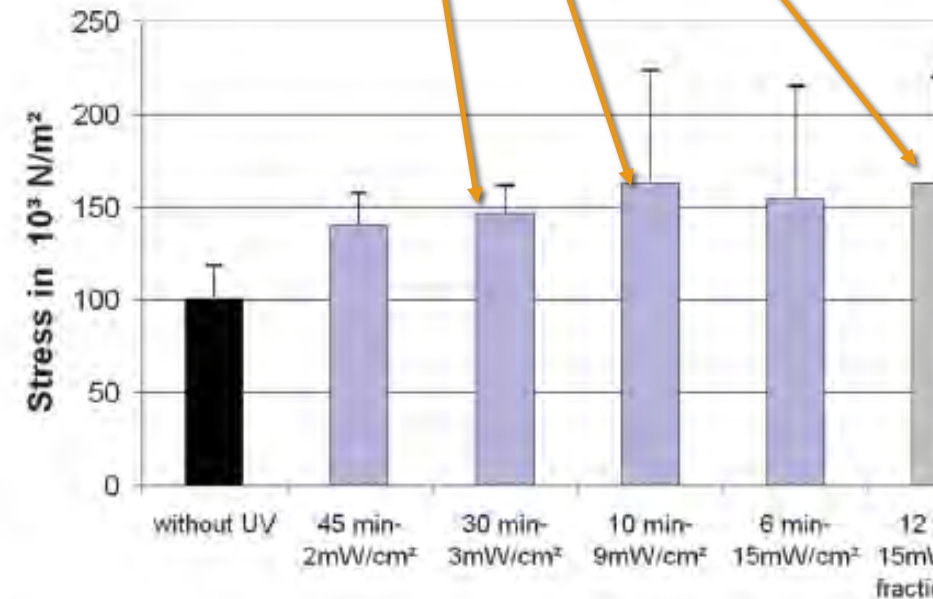
From the Physiological Laboratory, University of Cambridge

The Law Stated that Photochemical process in a tissue depends on the delivered and absorbed energy dose

$$\text{Effect (E Dose)} = I (\text{UV power}) \cdot t (\text{Exposure time})$$

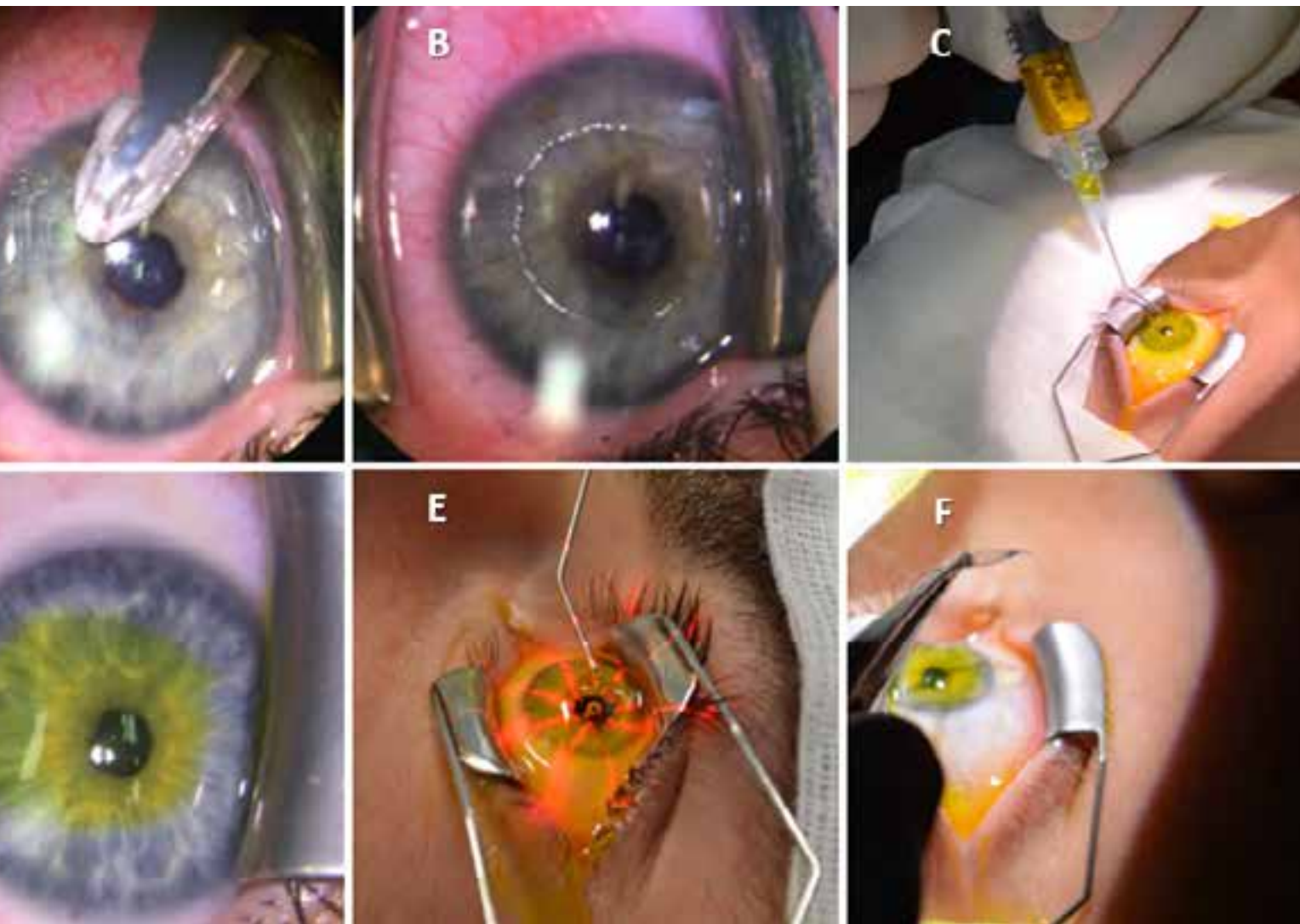
Delivering the same dose (5.4 J/cm²) 1 mW x 30 min - 9 mW x 10 min - 18 mW x 5 min, 15 mW x 6 min - 30 mW x 3 min

Theoretically the biological effect should be proportional to the total energy dose delivered in the tissue



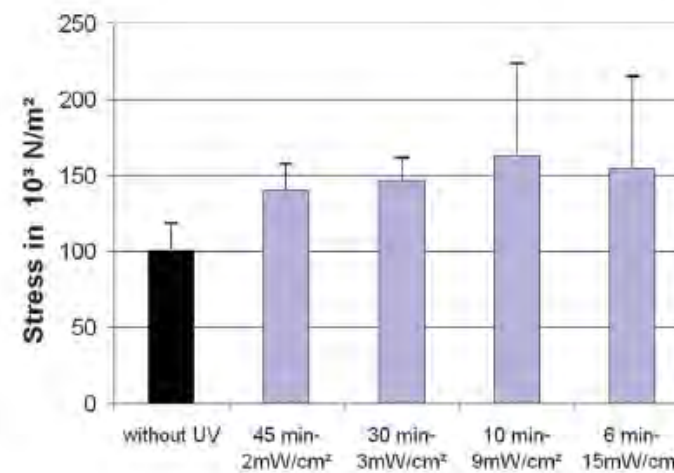
W-pulsed-light High-Irradiance Accelerated Crosslinking keratectomy: surgical technique and 2-year clinical results v Epi-Bowman keratectomy: surgical technique and 2-year clinical results

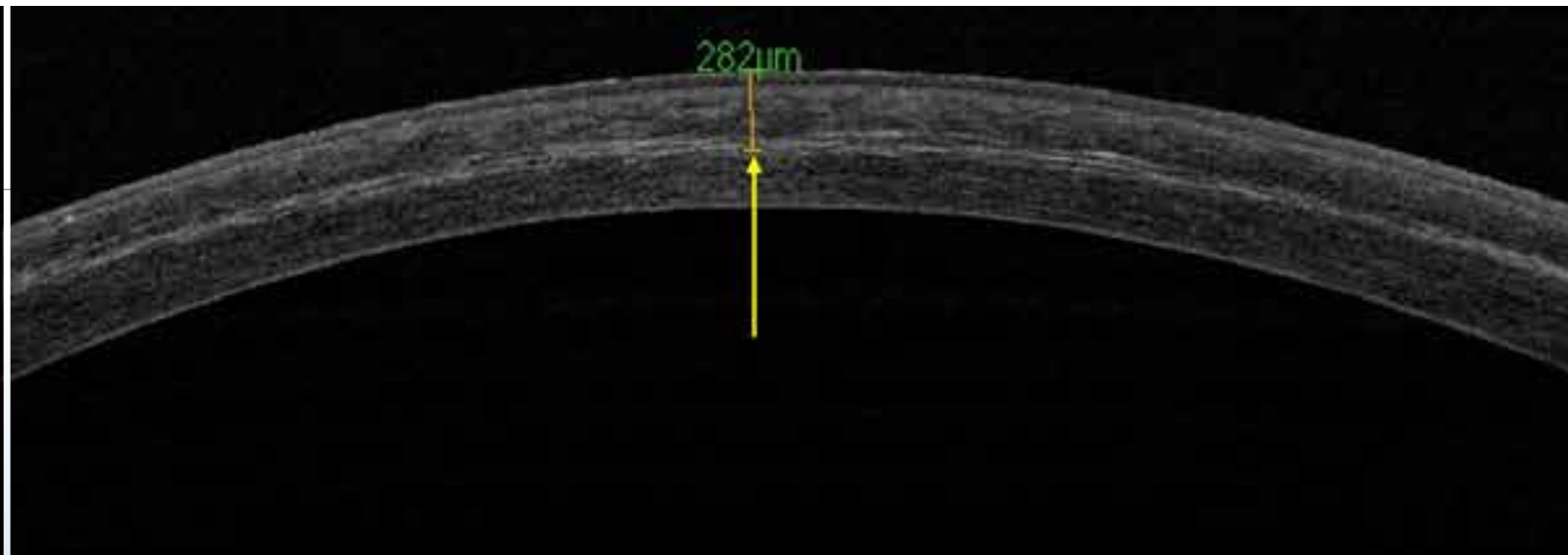
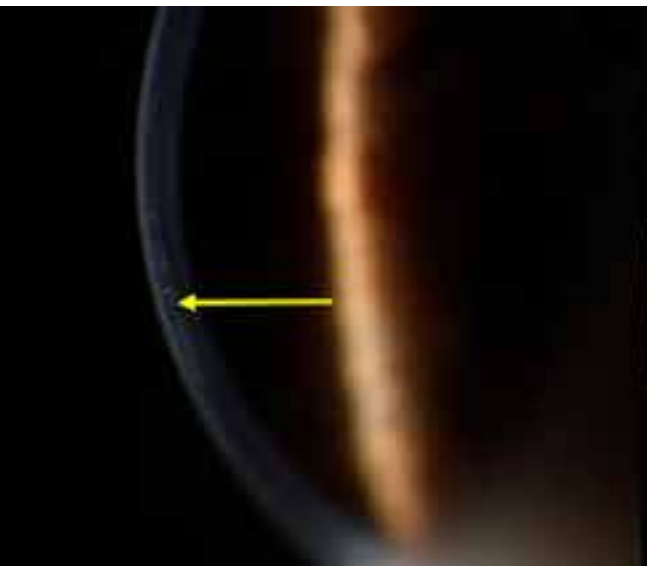
Mazzotta MD, PhD, Claudio Traversi MD, PhD, Simone Alex Bagaglia MD, 3 4 Alessandro Meduri MD, PhD, Miguel Rechichi MD, Ph



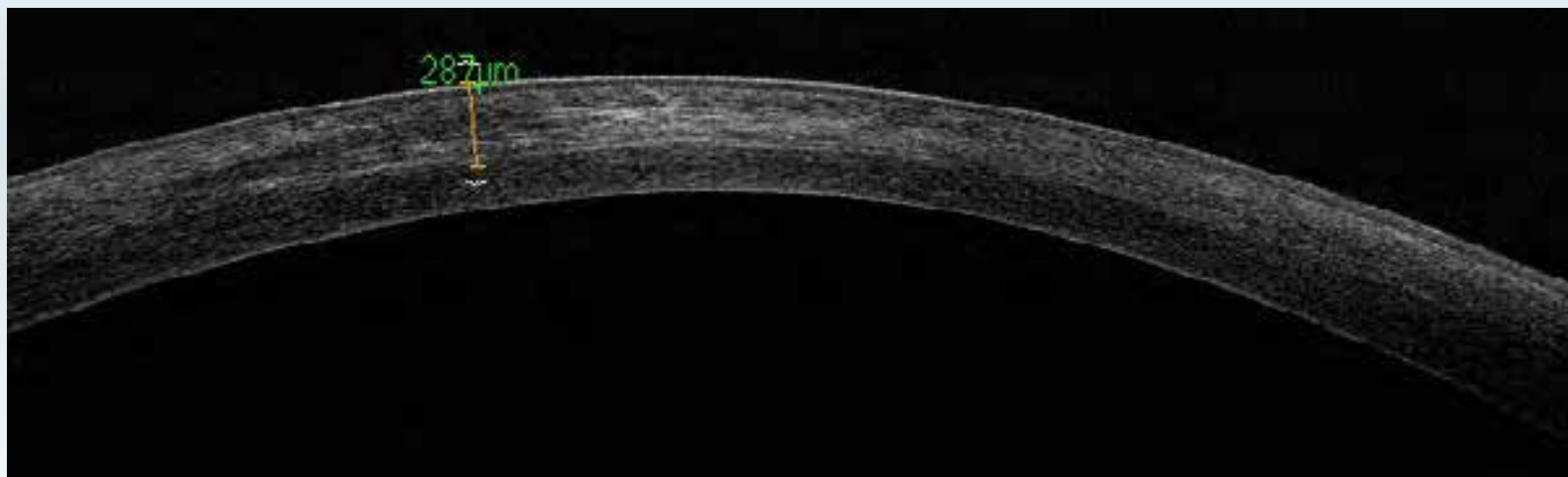
Submitted to JRS

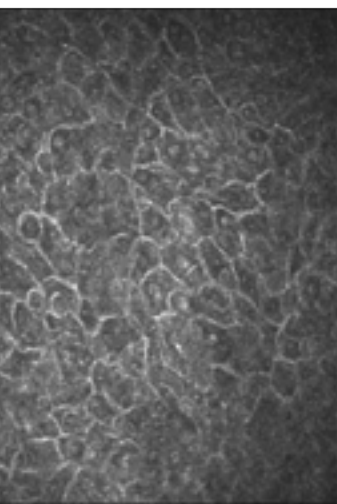
S.I.C.C. 15mW-HIXL



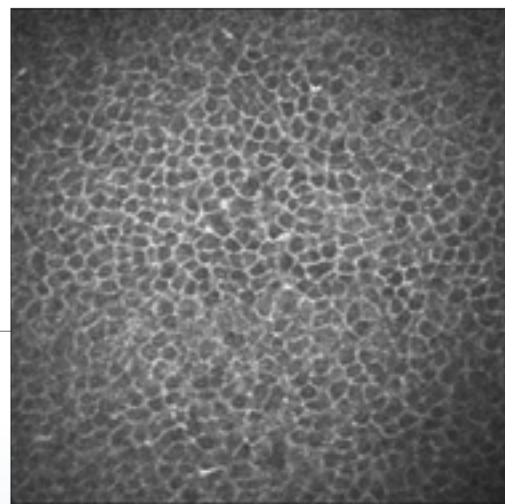


I.C.C. 15mW-HIXL

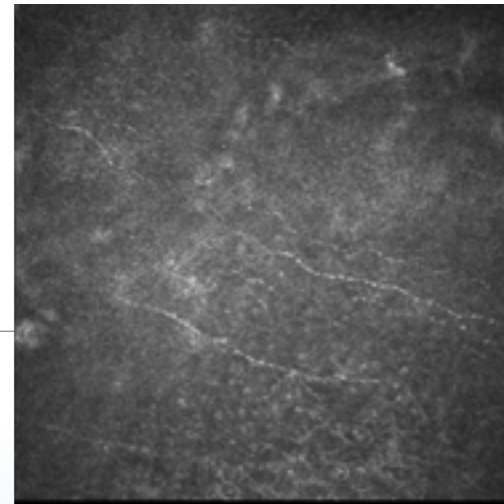




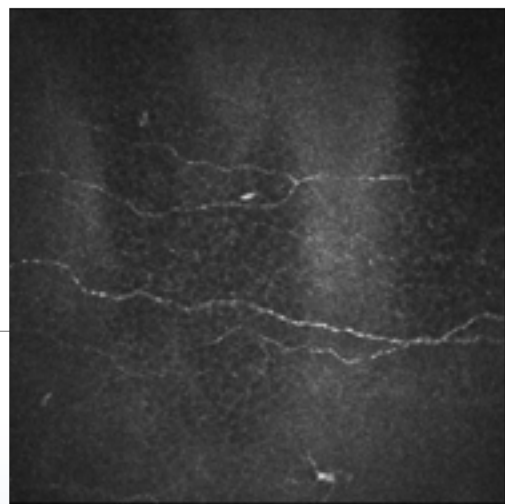
[0], 22/01/2016, OD
HEIDELBERG ENGINEERING



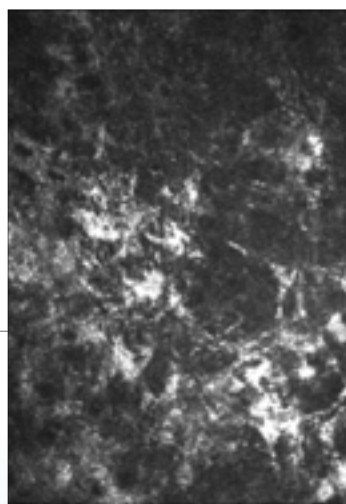
Cornea Section [65], 18/02/2016, OD
1 / 1: 20 μ m
HEIDELBERG ENGINEERING



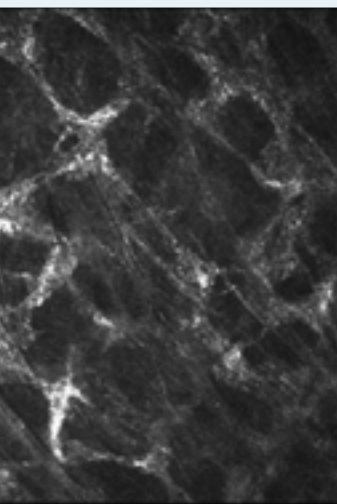
Cornea Section [189], 22/01/2016, OD
1 / 1: 23 μ m
HEIDELBERG ENGINEERING



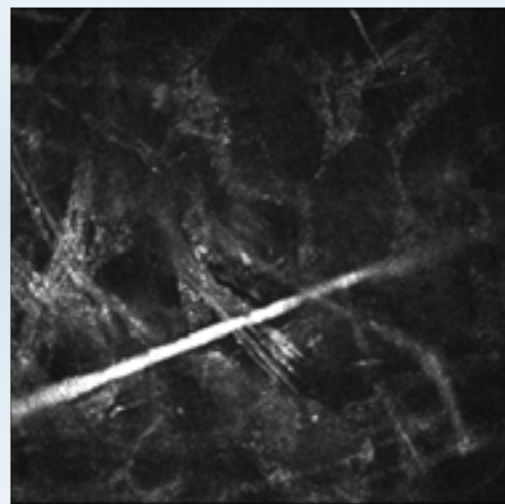
Cornea Section [7], 08/03/2016, OD
1 / 1: 37 μ m
HEIDELBERG ENGINEERING



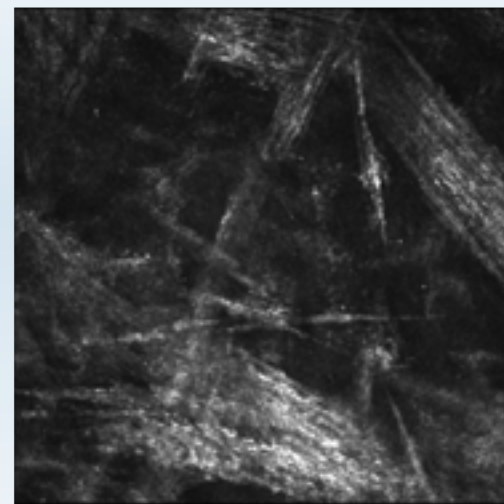
Cornea Section [9], 08/03/2016,
1 / 1: 47 μ m



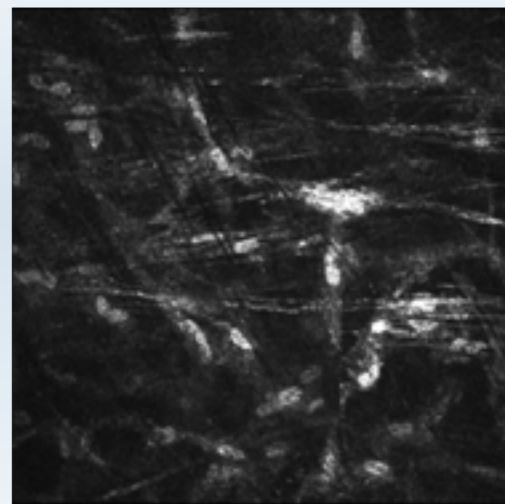
[32], 18/02/2016, OD
HEIDELBERG ENGINEERING



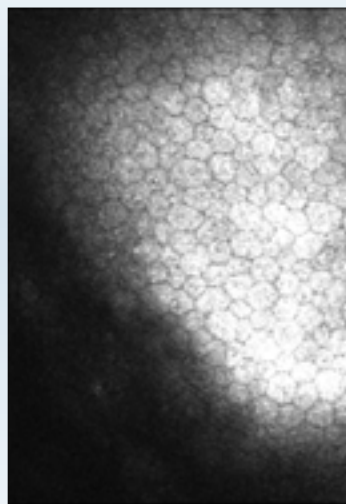
Cornea Section [39], 18/02/2016, OD
1 / 1: 208 μ m
HEIDELBERG ENGINEERING



Cornea Section [42], 18/02/2016, OD
1 / 1: 229 μ m
HEIDELBERG ENGINEERING



Cornea Section [47], 18/02/2016, OD
1 / 1: 326 μ m
HEIDELBERG ENGINEERING



Cornea Section [61], 08/03/2016,
1 / 1: 427 μ m

Mazzotta et al.: In vivo Confocal Microscopy Report after Lasik with Sequential Accelerated Corneal Collagen Cross-Linking Treatment

In vivo Confocal Microscopy Report after Lasik with Sequential Accelerated Corneal Collagen Cross-Linking Treatment

Cosimo Mazzotta^a Angelo Balestrazzi^a Claudio Traversi^a
Stefano Caragiuli^a Aldo Caporossi^b

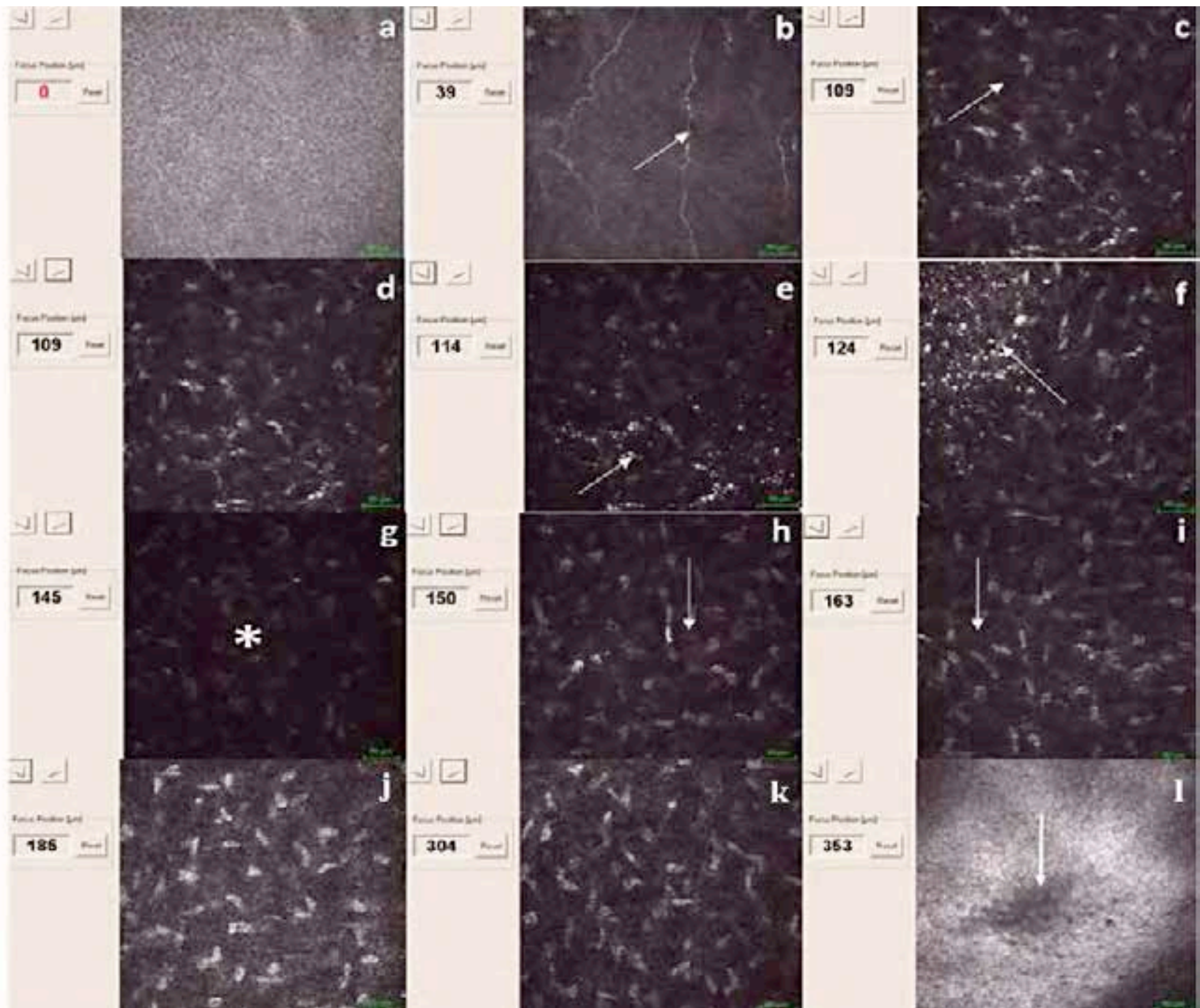
^aDepartment of Ophthalmology, Siena University Hospital, Siena, and ^bDepartment of Ophthalmology, Rome Catholic University, Rome, Italy

- Hyperopic
- High Myopia
- Thin Corneas

prophylactic customization of the biomechanical behavior of corneal collagen



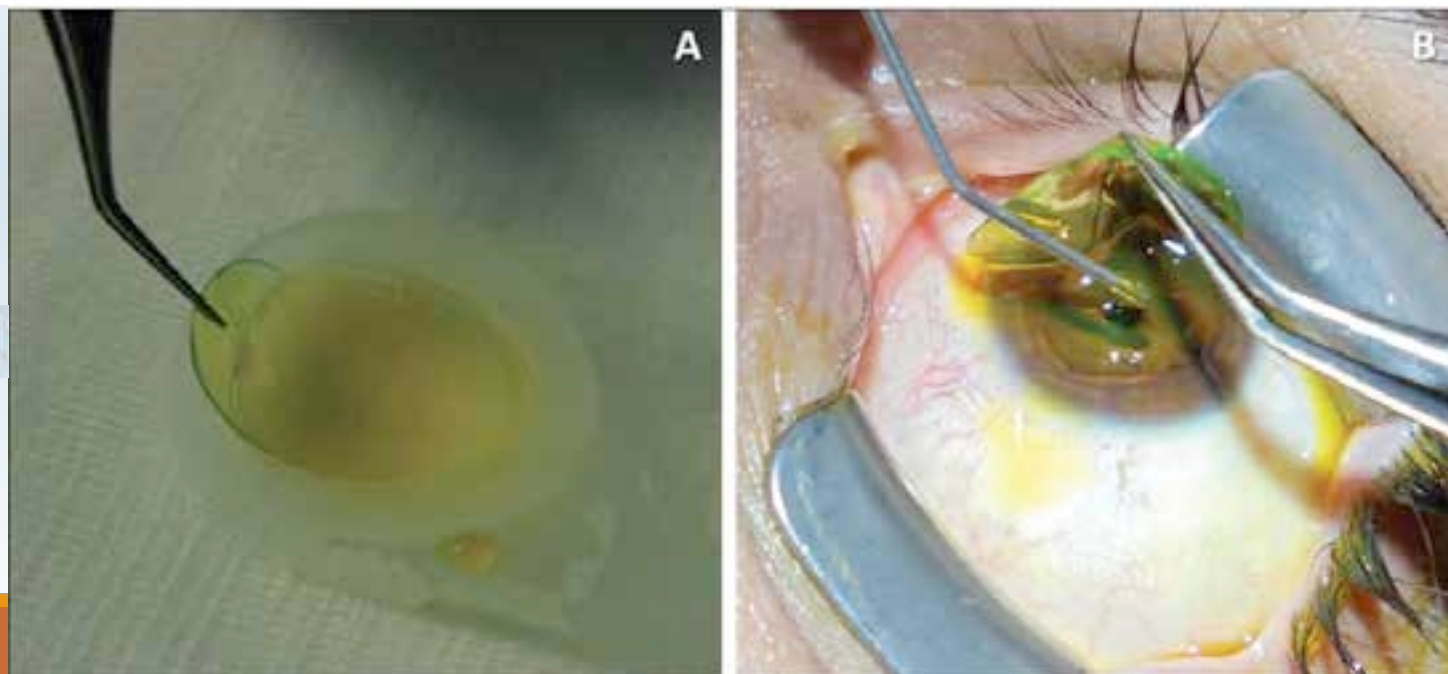
Lasik combined with sequential accelerated corneal collagen cross-linking



In Vivo Confocal Microscopy After Contact Lens-Assisted Corneal Collagen Cross-linking for Thin Keratoconic Corneas

Cosimo Mazzotta, MD, PhD; Soosan Jacob, MS, FRCS, DNB; Amar Agarwal, MS, FRCS, FRCOphth; Dhivya Ashok Kumar, MD

Refract Surg. 2016;32(5):326-331.]



IVCM for Contact Lens-Assisted CXL/Mazzotta et al

[*J Refract Surg.* 2016;32(5):326-331.]

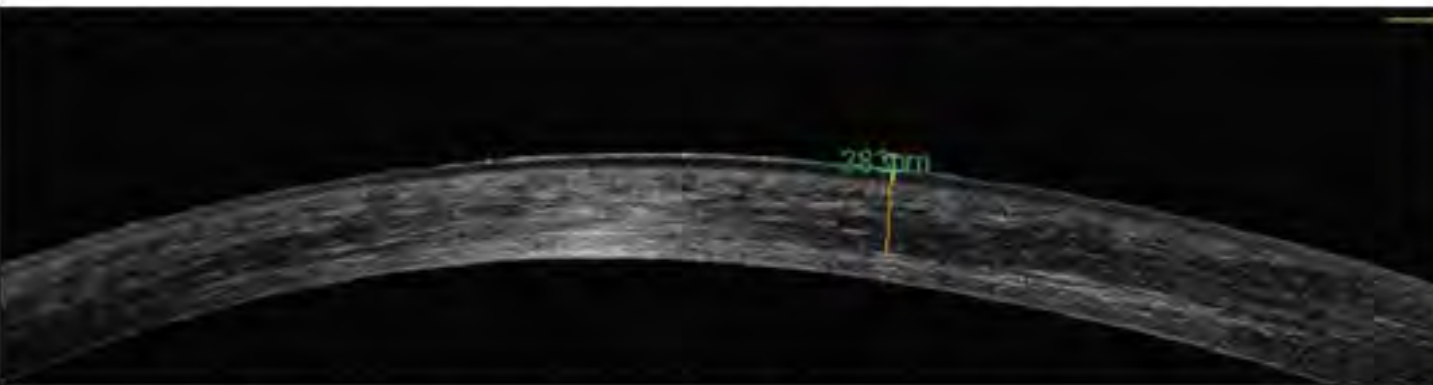


Figure 3. One-month postoperative anterior segment optical coherence tomography after contact lens-assisted corneal collagen cross-linking (3 mW/cm²; 5.4 J/cm²): epithelial thickness = 55 μ m, stromal demarcation line depth = 330 μ m. Preoperative thinnest point = 433 μ m, minimum stromal thickness without epithelium = 378 μ m.

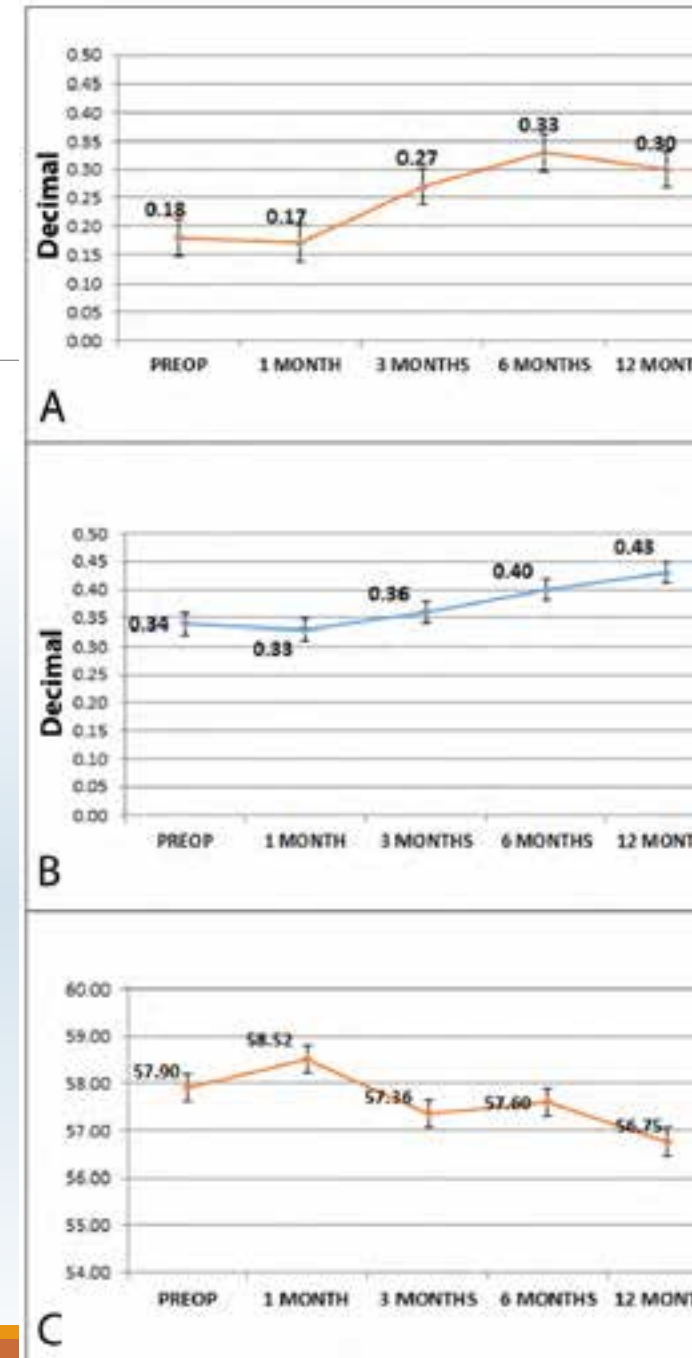
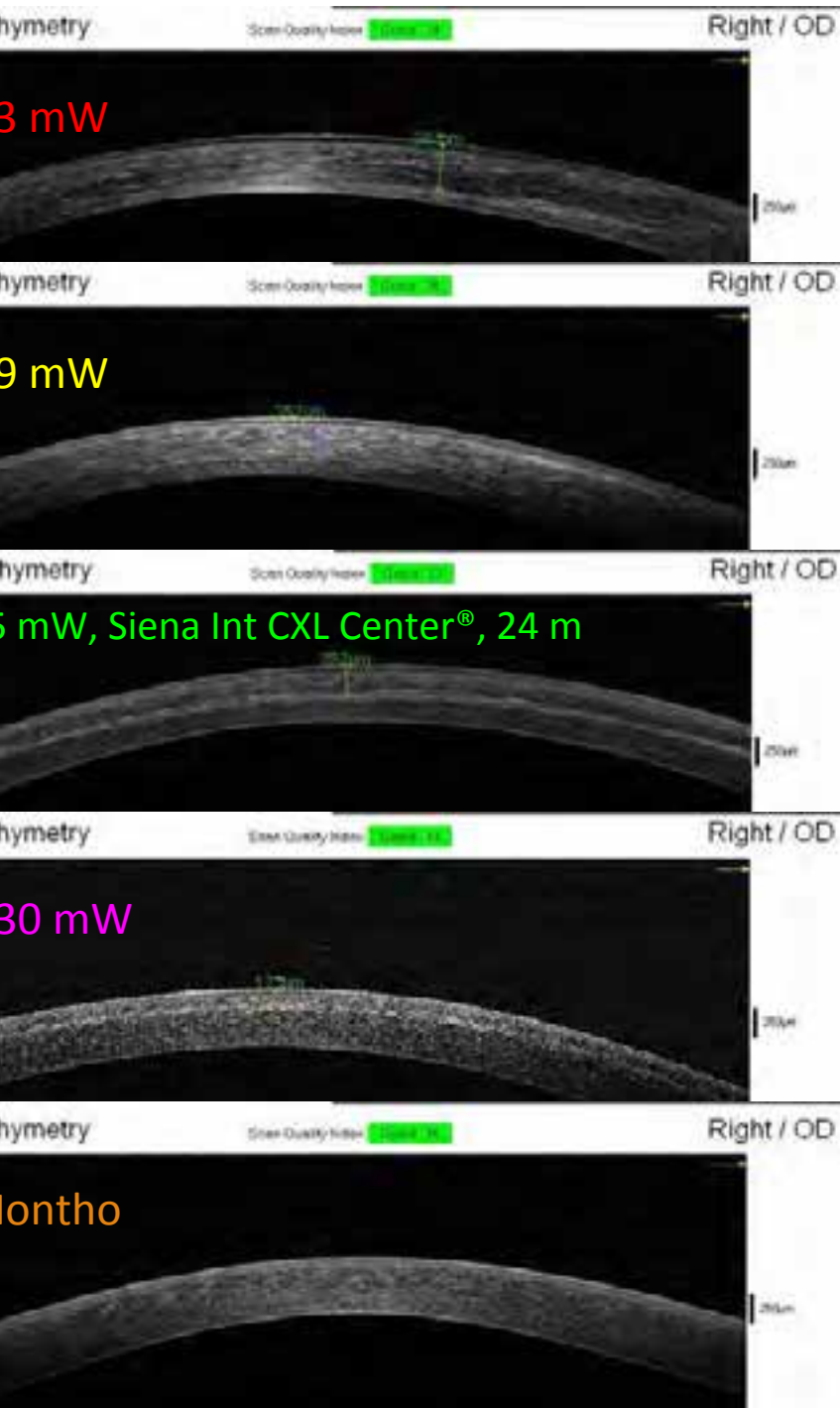


Figure 4. Preoperative and postoperative (A) uncorrected distance acuity, (B) corrected distance visual acuity, and (C) maximum keratometry.

Conclusions



- **DIFFERENT PROTOCOLS LEAD TO DIFFERENT STRUCTURAL CHANGES, PENETRATION AND EFFICACY!!!**
- **THIS OPEN THE WAY TO CUSTOMIZE EACH TREATMENT INCLUDING THIN CORNEAS**

Thank You for Attention

